Mixed-Mode GPS Network Processing for Deformation Monitoring Applications in the Equatorial Region

Volker JANSSEN and Chris RIZOS

School of Surveying and Spatial Information Systems
The University of New South Wales
Sydney NSW 2052, Australia
Ph: +61-2-93854208, Fax: +61-2-93137493, Email: v.janssen@student.unsw.edu.au

Abstract

The Global Positioning System (GPS) can be utilised in a wide range of deformation monitoring applications. During the past few years a methodology has been developed for processing data collected by GPS networks consisting of a mixed set of single-frequency and dual-frequency receivers. The strategy is to deploy a few permanent, 'fiducial' GPS stations with dual-frequency, geodetic-grade receivers surrounding an 'inner' network of low-cost, single-frequency GPS receivers. Such a configuration offers considerable flexibility and cost savings for deformation monitoring applications, which require a dense spatial coverage of GPS stations, and where it is not possible, nor appropriate, to establish permanent GPS networks using dual-frequency instrumentation.

The basis of the processing methodology is to separate the dual-frequency, 'fiducial' station data processing from the baseline processing involving the inner (single-frequency) receivers located in the deformation zone. The dual-frequency GPS network is used to generate a file of 'corrections', analogous to Wide Area DGPS correction models for the distance dependent biases. These 'corrections' are then applied to the double-differenced phase observations from the inner receivers to improve the baseline accuracies (primarily through empirical modelling of the residual atmospheric biases that otherwise would be neglected).

The performance of this configuration under severe ionospheric conditions in the equatorial region has been investigated by simulating such a two-stage network using data collected in the Hong Kong GPS Active Network. A description of the processing strategy, together with a discussion of the results, is presented.

1 Introduction

The Global Positioning System (GPS) can be utilised in a wide range of deformation monitoring applications. The decreasing cost of GPS hardware, together with the increased reliability of the technology, facilitates such demanding applications as the monitoring of active volcanoes, tectonic fault lines, landslides, ground subsidence, bridges, dams, high-rise buildings, etc. GPS deformation measurements can be continuous, automatic, conducted in all weather conditions, and provide three-dimensional positioning results. Higher computing power also means that the complex mathematics required to process GPS baselines can be easily handled in near real-time.

Deformation monitoring using GPS is usually carried out by installing and operating a local network of GPS receivers located on and around the deforming body. One of the first *continuous* GPS networks was established in March 1988 on the Izu Peninsula in central Japan to support earthquake prediction research. Daily observations of this network led to the first GPS measurements of surface deformation as they occurred. Shimada et al. (1990) reported that, "We have, for the first time, used GPS fixed-point measurements to follow the evolution with time of the crustal movements; such measurements provide a continuous uninterrupted record of deformation." Numerous continuous GPS networks of different size have since been established on tall buildings (Celebi & Sanli, 2002; Ogaja et al., 2001), bridges (Ashkenazi et al., 1997; Wong et

al., 2001), dams (Behr et al., 1998; Whitaker et al., 1998), volcanoes (Dixon et al., 1997; Owen et al., 2000), and on tectonic faults (Hudnut et al., 2001; Tsuji et al., 1995).

However, these networks are comparatively costly because they rely entirely on the use of high-quality dual-frequency instrumentation. In order to keep the cost of such a deformation monitoring system to a minimum, single-frequency GPS receivers need to be used. On the other hand, some atmospheric biases (mainly the ionospheric delay) cannot be accounted for directly if only one frequency is used. A single-frequency, carrier phase-tracking system is considered appropriate for small-scale continuous GPS networks if the baseline lengths are not longer than 10 kilometres. This 'rule-of-thumb' implies that the differential ionospheric and tropospheric delay between the two receivers is essentially zero, and therefore does not impact on the baseline result. Orbit bias over such short distances can be largely ignored (Rizos, 1997). Presently, however, with the current solar sunspot cycle maximum, ionospheric disturbances have indeed corrupted L1 baseline measurements over distances less than 10km, adversely affecting baseline repeatability (see, e.g., Janssen et al., 2001). This problem is very much pronounced in equatorial regions, areas prone to highly disturbed ionospheric conditions. It is therefore necessary to combine a single-frequency deformation monitoring network with a small number of dual-frequency receivers in order to account for these atmospheric effects. This methodology leads to a *mixed-mode* deformation monitoring system that is both cost-effective *and* accurate. Meertens (1999) reports on a single-frequency system for volcano deformation monitoring at the Long Valley Caldera, USA, and Mt. Popocatepetl, Mexico, which is soon to be augmented with the addition of a small number of dual-frequency receivers for atmospheric modelling. Hartinger & Brunner (2000) describe a mixed-mode approach to monitor landslides in the Austrian Alps.

In this paper a fiducial network of three dual-frequency GPS receivers surrounding the deformation zone is used to generate empirical 'correction terms' (Rizos et al., 1998; 2000). These double-differenced corrections are then applied to the data from the single-frequency baselines in the inner network to account for residual atmospheric biases. In this paper, the ionospheric correction model proposed for this mixed-mode system and the data processing strategy are described, and experimental results obtained in an equatorial region, are presented.

2 Ionospheric Corrections

The ionosphere is part of the Earth's upper atmosphere stretching from a height of about 50km to 1000km above the surface. The high spatial and temporal variability of the ionosphere has a major effect on GPS signals travelling from the satellite to the receiver. Moreover, the condition of the ionosphere is strongly related to the 11-year sunspot activity cycle. The most recent solar maximum occurred in 2000-2001, causing high ionospheric activity and having a clear impact on the results presented in this paper.

It is well known that the ionosphere is most active in a band extending up to approximately 20° on either side of the geomagnetic equator. This is also one of the two regions where small-scale ionospheric disturbances (scintillations) mainly occur. The other being the high-latitude region close to the poles. (Scintillations are short-term signal variations in amplitude and phase.) In the equatorial region scintillations occur between approximately one hour after sunset until midnight (Klobuchar, 1996), and should have disappeared by 3am local time (IPS, 2000). The occurrence of scintillations also varies with the seasons. Between April and August they are less severe in the American, African and Indian longitude regions, but are at a maximum in the Pacific region, while the situation is reversed from September to March (Seeber, 1993). In mid-latitudes scintillations are rarely experienced, but Medium-Scale Travelling Ionospheric Disturbances (MSTIDs) occur frequently, mainly during daytime in the winter months, during periods of high solar activity, with a maximum around local noon (Wanninger, 1999).

While data from dual-frequency receivers can account for the ionospheric delay directly by the appropriate linear combination of measurements made on both frequencies, data from single-

frequency receivers cannot be corrected in this way. For deformation monitoring applications, a fiducial network of three dual-frequency receivers surrounding the deformation zone can be used to generate 'correction terms', which can then be applied to the single-frequency observations to account for these effects.

Such a fiducial network should ideally surround the inner single-frequency network, as described by Han (1997). Figure 1 shows the ideal network configuration where the triangles denote fiducial stations, while the dots indicate single-frequency sites. The fiducial reference stations are to be situated outside the deformation zone but within the local tectonic region in order to avoid unwanted displacements of the external network.

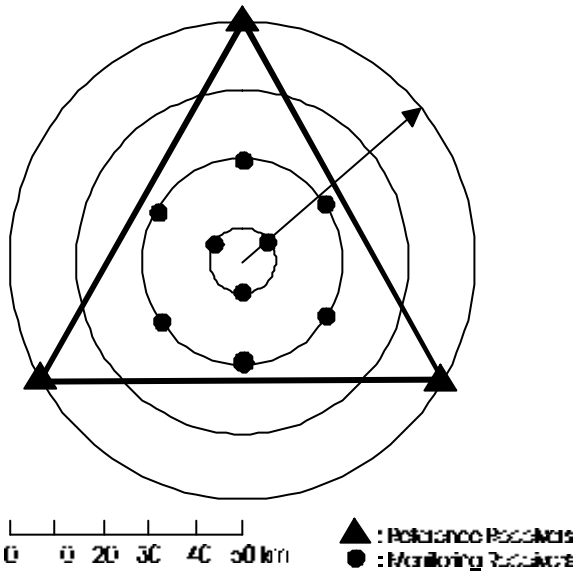

Figure 1: Ideal network configuration of a mixed-mode GPS deformation monitoring network

Han & Rizos (1996) and Han (1997) have proposed a linear combination model, which utilises a single ionospheric layer model at a height of 350km. This approach can account for orbit bias and ionospheric delay, as well as mitigate tropospheric delay, multipath and measurement noise across the network. Data from the fiducial GPS reference station network can be used to derive empirical corrections to the double-differenced carrier phase data formed between the stations of the inner network. The procedure is described in Chen et al. (2001a) and summarised below.

The double-differenced observable can be written as (Ibid, 2001a):

$$\nabla\Delta f = \nabla\Delta r + \nabla\Delta dr + l \cdot \nabla\Delta N - \nabla\Delta d_{ion} + \nabla\Delta d_{trop} + \nabla\Delta d^{j}_{mp} + e_{\nabla\Delta f} \qquad (1)$$

where $\nabla\Delta$ = double-difference operator
ϕ = carrier phase observation in units of metres
ρ = distance between receiver station and satellite
d = effect of satellite ephemeris error on a particular receiver-satellite range
λ = wavelength of the carrier phase
N = integer ambiguity for a particular satellite-receiver phase measurement
d_{ion}, d_{trop}, d^{φ}_{mp} = ionospheric delay, tropospheric delay, multipath effect
$\varepsilon_{\nabla\Delta\phi}$ = carrier phase observation noise in the one-way observation

Assume the number of GPS reference stations is three. For a baseline between one of these reference stations and a single-frequency user receiver located inside the triangle (denoted by u), the above equation can then be expressed in the form of a linear combination (Han, 1997):

$$\nabla\Delta f_{u,3} - \left[a_1 \cdot V_{1,3} + a_2 \cdot V_{2,3}\right] = \nabla\Delta r_{u,3} + l \cdot \nabla\Delta N_{u,3} + e_{\nabla\Delta f_{u,3}} \quad (2)$$

The parameters α_i refer to the position of the user receiver inside the fiducial triangle and can be determined based on the conditions given in Han & Rizos (1996) and Wu (1994):

$$\sum_{i=1}^{3} a_i = 1,\ \sum_{i=1}^{3} a_i \cdot \left(\vec{X}_u - \vec{X}_i\right) = 0 \text{ and } \sum_{i=1}^{3} a_i^2 = min \quad (3)$$

where $\vec{X}_u$ = user station position vector and $\vec{X}_i$ = reference station position vector.

The residual vectors are formed from the double-differenced observations between reference stations 1 & 3 and 2 & 3:

$$V_{1,3} = \nabla\Delta f_{1,3} - \nabla\Delta N_{1,3} - \nabla\Delta r_{1,3} \quad (4)$$

$$V_{2,3} = \nabla\Delta f_{2,3} - \nabla\Delta N_{2,3} - \nabla\Delta r_{2,3} \quad (5)$$

The correction term $\left[a_1 \cdot V_{1,3} + a_2 \cdot V_{2,3}\right]$ can now be determined. If the baseline between two GPS stations j and k of the inner network is considered, the linear combination can be written as:

$$\nabla\Delta f_{k,j} - \left[a_1^{k,j} \cdot V_{1,3} + a_2^{k,j} \cdot V_{2,3}\right] = \nabla\Delta r_{k,j} + l \cdot \nabla\Delta N_{k,j} + e_{k,j} \quad (6)$$

where $\alpha_i^{k,j}$ = difference in the α_i value for stations j and k.

By forming the double-differenced observables between the inner single-frequency receivers, and using the residual vectors generated from the fiducial reference stations, the inner stations' coordinates can be determined without the need to use any GPS reference station observations at all. In practice, holding one fiducial site fixed, the baselines to the other two sites are processed and 'correction terms' are obtained for both baselines. These are then scaled (by means of the parameters α) according to the position of the inner stations inside the fiducial triangle to generate double-differenced corrections for the inner baselines.

The nature of these empirically-derived double-differenced 'correction terms' has been investigated by Janssen et al. (2001). A range of GPS data sets were processed incorporating a variety of baseline lengths, different geographical locations and different periods of sunspot activity (and hence ionospheric conditions). The standard deviation of the double-differenced 'correction terms' was found to be increasing linearly with increasing baseline length. The rate of increase was much more severe under solar maximum conditions as opposed to periods of low solar activity. This suggests that long baselines between reference stations might not be capable of generating reliable corrections under these conditions. However, the magnitudes of these biases are not entirely a function of distance, hence it is difficult to predict what should be the dimensions of the reference station network that would faithfully model the distance dependent biases. The geographic location of the network is certainly another contributing factor, as the ionospheric effects for GPS sites in the equatorial region are much larger compared to mid-latitude sites.

3 Single-Frequency Data Processing

A single-frequency version of the Baseline software package developed at UNSW is used to process the inner network. For deformation monitoring applications multi-baseline processing strategies should be used because all baselines are then computed together, taking into account the between-baseline correlations which arise from observing a GPS network simultaneously (Craymer & Beck, 1992). For continuous deformation monitoring a near real-time, epoch-by-epoch solution is desired in order to detect movements over a short period of time.

In a number of deformation monitoring applications, such as local networks around active volcanoes or dams, the deforming body itself will obstruct part of the sky. If the usual base-station / base-satellite approach is used in the data processing, only the common satellites are considered. This results in the number of possible double-differences being comparatively low, hence a lot of potentially valuable information can be lost. As described in Janssen (2001), the Baseline software utilises a procedure to optimise the number of double-differenced observations used in the data processing. This method considers satellites that are visible from a small number of network stations only. Hence, the number of independent double-differenced observables can be maximised in order to generate a more accurate and reliable solution. This data processing approach determines the receiver-to-satellite connections for each site of the network. A maximum set of independent double-differenced combinations is then computed using vector space methods and the geometric characterisations of Boolean matrices, as suggested by Saalfeld (1999).

4 Experimental Data

Data from the Hong Kong GPS Active Network (Chen et al., 2001b) were used to investigate the performance of such a network configuration in low-latitude regions. Figure 2 shows the location of the GPS sites, which are all equipped with dual-frequency receivers. The network consists of an outer network of three sites (HKKY, HKFN, HKSL) surrounding two inner sites (HKKT, HKLT). The outer sites were used as fiducial GPS reference stations, indicated by triangles in Figure 2, while the inner sites (indicated by circles) simulated single-frequency receiver stations (by ignoring the observations made on L2). Due to the absence of a third site within the fiducial triangle, the fiducial site HKKY was used to form the inner (single-frequency) baselines. Note that HKLT is located just outside the fiducial triangle, which should normally be avoided. However, this does not have any effect on the processing in this case, as HKKY-HKFN and HKKY-HKSL are used as fiducial baselines. The data were collected under solar maximum conditions, using an observation rate of 30 seconds, on three consecutive days from 11-13 October 2000 (DOY 285-287).

The WGS84 coordinates of the GPS network stations are shown in Table 1. These coordinates were taken from a global solution of a survey campaign spanning several days, which was generated by A/Prof. Peter Morgan at the University of Canberra using the GAMIT software and precise ephemerides (Morgan, 2002, personal communication).

Table 1: WGS84 coordinates of the GPS network stations located in Hong Kong

Site	HKKY	HKFN	HKSL
Latitude (N)	22° 17’ 02.6499’’	22° 29’ 40.8696’’	22° 22’ 19.2165’’
Longitude (E)	114° 04’ 34.5651’’	114° 08’ 17.4086’’	113° 55’ 40.7355’’
Height [m]	113.975	41.173	95.261

Site	HKKT	HKLT
Latitude (N)	22° 26’ 41.6614’’	22° 25’ 05.2822’’
Longitude (E)	114° 03’ 59.6371’’	113° 59’ 47.8470’’
Height [m]	34.532	125.897

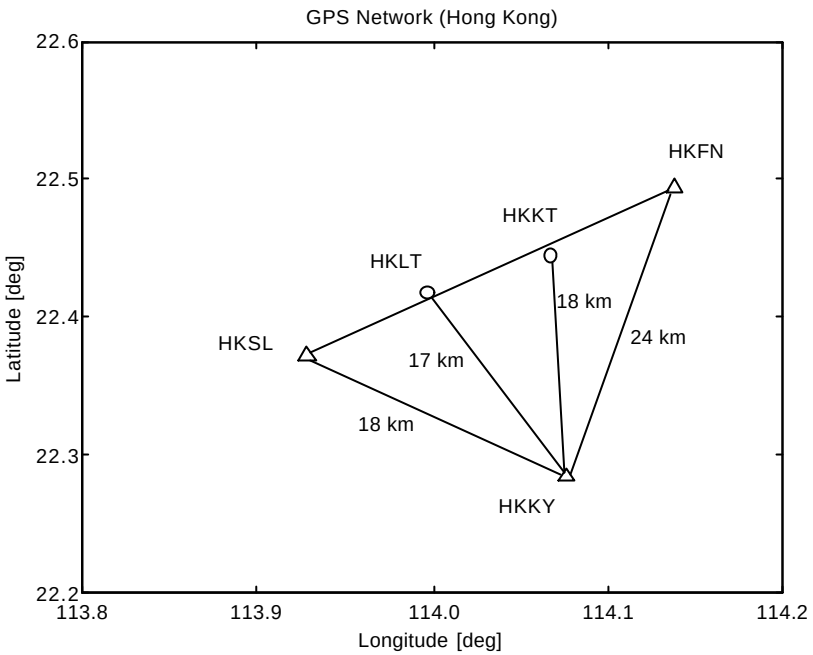

Figure 2: Hong Kong GPS Active Network stations used in this study

4.1 Ionospheric Corrections for the Fiducial Baselines

Processing the dual-frequency data with a modified version of the Bernese software, ionospheric L1 correction terms were determined for four baselines on three successive days. The baselines HKKY-HKFN (24km) and HKKY-HKSL (18km) were used as fiducial reference baselines. For comparison, corrections were also obtained for the inner baselines HKKY-HKKT (18km) and HKKY-HKLT (17km) using observations made on both frequencies. Figures 3, 5 and 7 show the double-differenced corrections obtained for the fiducial baselines on L1 for three consecutive 24-hour observation sessions, while Figures 4, 6 and 8 show the corrections obtained for the inner baselines. Table 2 shows several parameters characterising the correction terms, i.e. the minimum, maximum and mean corrections, their standard deviations and the number of double-differences involved.

It can be seen that, as expected, ionospheric activity in the equatorial region is at its peak between sunset and 2am local time. However, a lot of activity is also evident during daylight hours. This may be explained by intensified small-scale disturbances in the ionosphere during a period of increased solar activity. Furthermore, it can be identified as the primary diurnal maximum of the equatorial anomaly, also known as the 'fountain effect' (high electron concentration observed on either side of the geomagnetic equator at magnetic latitudes of around 10-20°). Huang & Cheng (1991) state that the daily equatorial anomaly generally begins to develop at around 9-10am local time, reaching its primary maximum development at 2-3pm local time. In periods of solar maximum conditions, however, the anomaly is prone to peak after sunset, and gradients in the total electron content (TEC) are considerably larger at this secondary diurnal maximum (Skone, 2000). Horizontal gradients of up to $30 \cdot 10^{16}$ electrons per m^2 (30 TECU) have been observed in equatorial regions under solar maximum conditions (Wanninger, 1993).

Obviously the ionosphere was a little less active on day 287 compared to the two preceding days. The correction terms for all baselines show a similar pattern, but also reveal a distinct gradient of the ionospheric conditions. The magnitude of the ionospheric effect increases in the general direction from the southwest to the northeast, as indicated by the minimum and maximum correction terms and their standard deviation in Table 2. Note that the baselines considered are of approximately the same length, ranging from 17-24 km. The magnitude of the correction terms reaches values of more than two metres in some cases, which is rather surprising for such short

baselines, and initially raised questions of the reliability of the corrections. However, the results presented below prove that the corrections obtained here are indeed capable of improving baseline accuracy. Clearly, the ionospheric activity was extremely severe during the time of observation, hence significantly affecting GPS measurements.

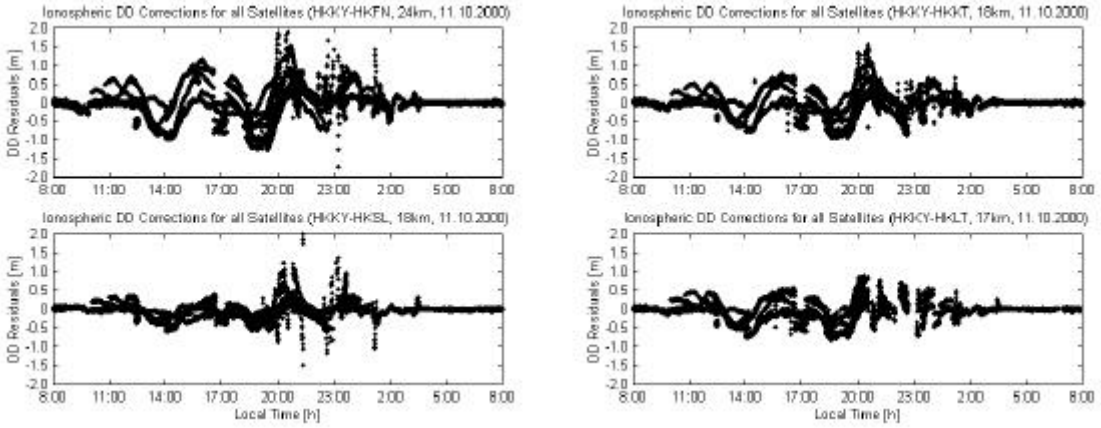

Figure 3+4: Double-differenced L1 corrections for fiducial (left) and inner (right) baselines (DOY 285)

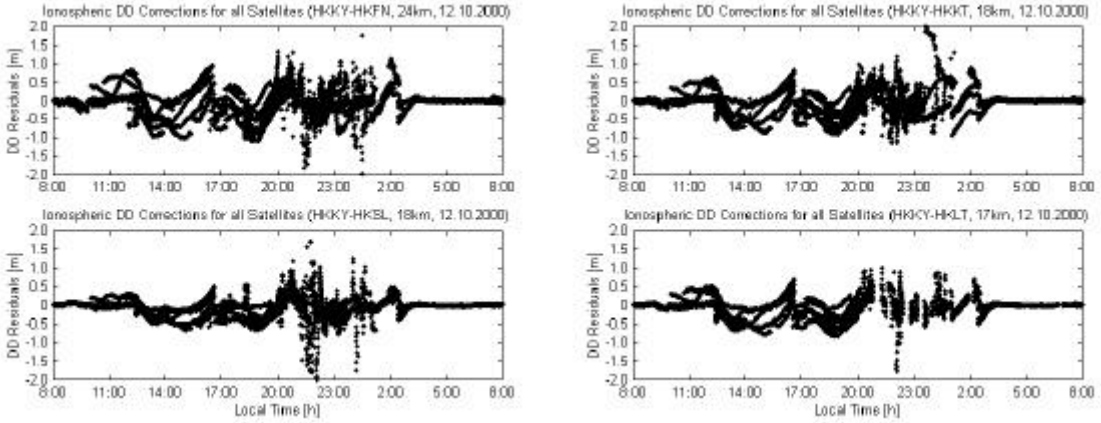

Figure 5+6: Double-differenced L1 corrections for fiducial (left) and inner (right) baselines (DOY 286)

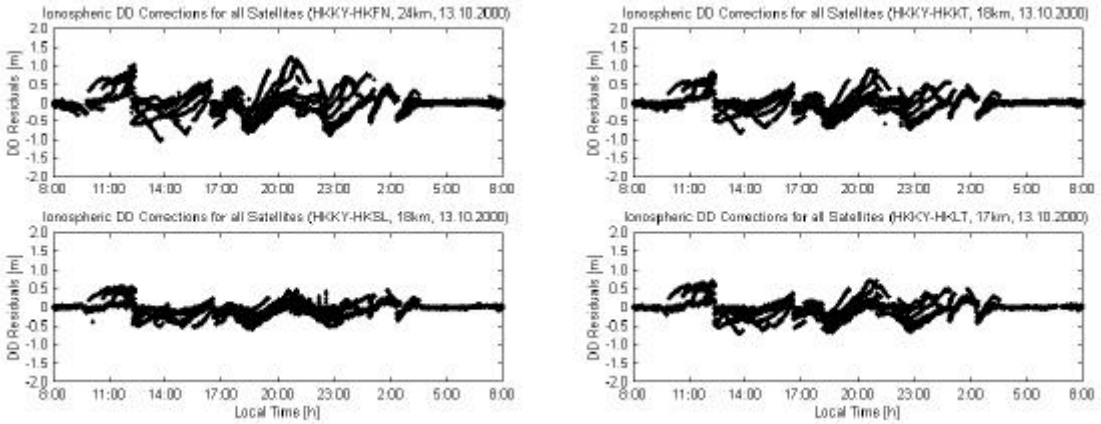

Figure 7+8: Double-differenced L1 corrections for fiducial (left) and inner (right) baselines (DOY 287)

Table 2: Double-differenced L1 corrections for different baselines

Baseline	D [km]	min [m]	max [m]	mean [m]	STD [m]	#DD
HK 11.10.2000 (L1)						
HKKY-HKFN	24	-1.71213	2.48976	-0.00822	0.42431	15336
HKKY-HKSL	18	-1.50008	2.05149	-0.04926	0.20338	15324
HKKY-HKKT	18	-0.94597	1.55869	-0.03585	0.32135	15457
HKKY-HKKT*	18	-0.95862	1.54679	-0.02357	0.31403	14980
HKKY-HKLT	17	-0.82337	0.88664	-0.04275	0.26003	13765
HKKY-HKLT*	17	-0.81494	1.59456	-0.03768	0.26240	14980
HK 12.10.2000 (L1)						
HKKY-HKFN	24	-2.22837	1.75940	-0.07406	0.35523	15340
HKKY-HKSL	18	-2.05571	1.70337	-0.07584	0.23511	15303
HKKY-HKKT	18	-1.13888	2.27508	-0.05846	0.33285	15381
HKKY-HKKT*	18	-1.17069	1.11037	-0.07131	0.27568	15054
HKKY-HKLT	17	-1.77687	0.98961	-0.08573	0.25912	13335
HKKY-HKLT*	17	-1.59388	1.21132	-0.07871	0.25588	15054
HK 13.10.2000 (L1)						
HKKY-HKFN	24	-1.02140	1.21435	0.00573	0.32181	16237
HKKY-HKSL	18	-0.57189	0.56004	-0.03961	0.18332	16127
HKKY-HKKT	18	-0.80377	0.88314	-0.00920	0.25847	16262
HKKY-HKKT*	18	-0.80317	0.88367	-0.00973	0.25514	16024
HKKY-HKLT	17	-0.70827	0.70789	-0.02482	0.23419	15638
HKKY-HKLT*	17	-0.69860	0.69954	-0.02541	0.22962	16024
* calculated using α values						

4.2 Ionospheric Corrections for the Inner Baselines

According to the procedure described in section 2, the parameters α were derived in order to relate the position of the inner network sites to the fiducial baselines. Table 3 lists the α values obtained for the inner GPS sites, α_1 and α_2 indicating the values corresponding to the fiducial baselines HKKY-HKFN and HKKY-HKSL respectively.

Table 3: α values obtained for the inner GPS network stations

Site	α_1	α_2
HKKT	0.627043	0.327184
HKLT	0.351097	0.683660

The L1 correction terms for the inner baselines can then be determined by forming the linear combination according to equation (2). Note that for a single-frequency GPS network located entirely inside the fiducial triangle, equation (6) would be used. Hence, the double-differenced correction terms for the inner baselines could be derived in two different ways. Firstly, as described in the previous section, the corrections were determined directly using dual-frequency data and the modified Bernese software (Figures 4, 6 and 8). Secondly, they were obtained indirectly by forming a linear combination of the corrections for the fiducial baselines using α values (Figures 9-11). Several parameters characterising these correction terms are shown in Table 2 (indicated by asterisks). It can be seen that the results are very similar and hence model the condition of the ionosphere very well. This indicates that the proposed procedure indeed generates the correct correction terms for the inner baselines.

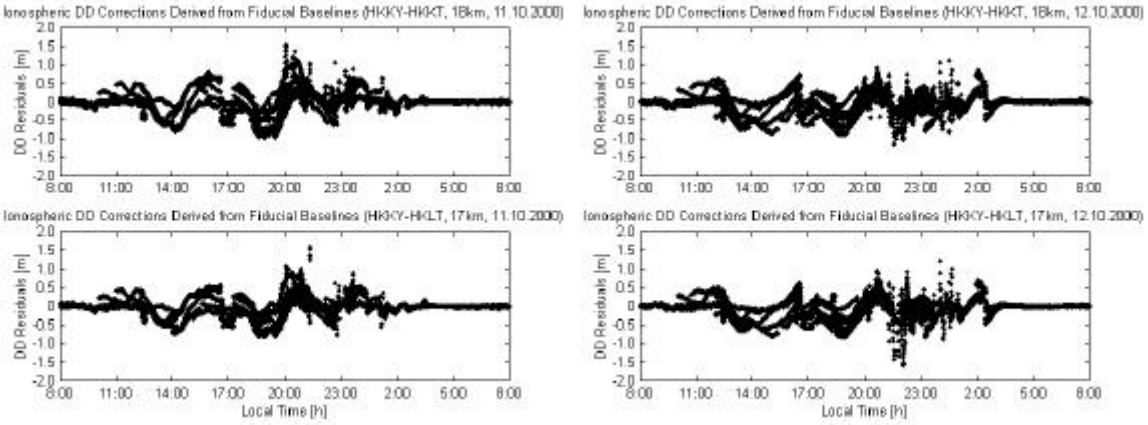

Figure 9+10: Double-differenced L1 corrections for the inner baselines obtained using α values (DOY 285+286)

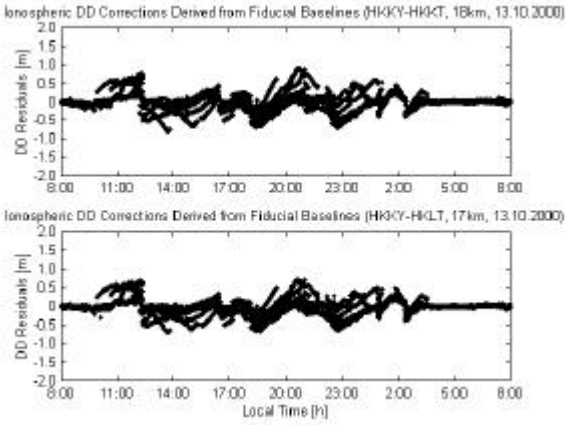

Figure 11: Double-differenced L1 corrections for the inner baselines obtained using α values (DOY 287)

4.3 Baseline Results

The Baseline software developed at UNSW is used to process the inner baselines in single-frequency mode with and without using ionospheric correction terms. It can readily be assumed that no ground deformation has taken place during the time of observation. Hence, the baseline repeatability gives a good indication of the accuracy that can be achieved for a GPS network located in close proximity to the geomagnetic equator with the method described in this paper. Figures 12-14 show the results obtained for the inner baselines using the Baseline software without applying ionospheric corrections, while Figures 15-17 show the results obtained after applying ionospheric corrections. The graphs show the Easting, Northing and Height components over a 24-hour period on three successive days, each dot representing a single-epoch solution. In both cases the Saastamoinen model was used to account for the tropospheric bias, as recommended by Mendes (1999).

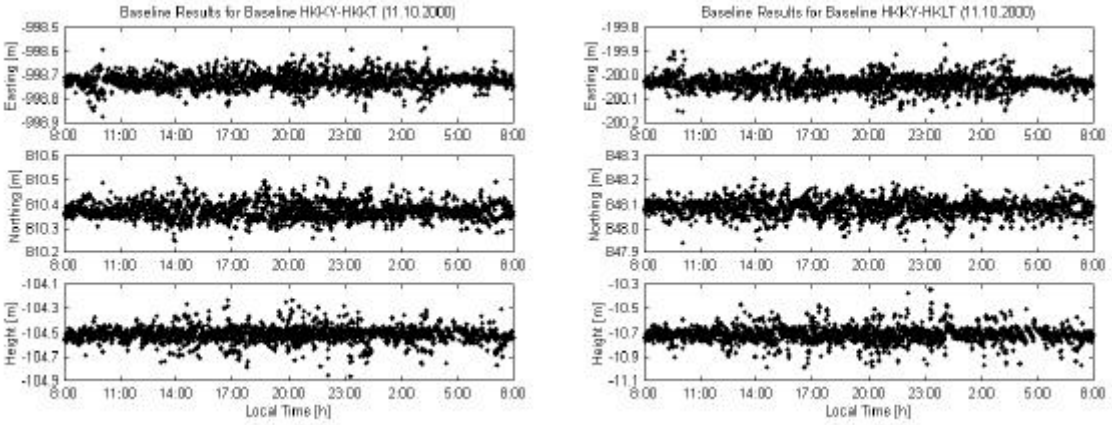

Figure 12: Results for the inner baselines not using ionospheric corrections (DOY 285)

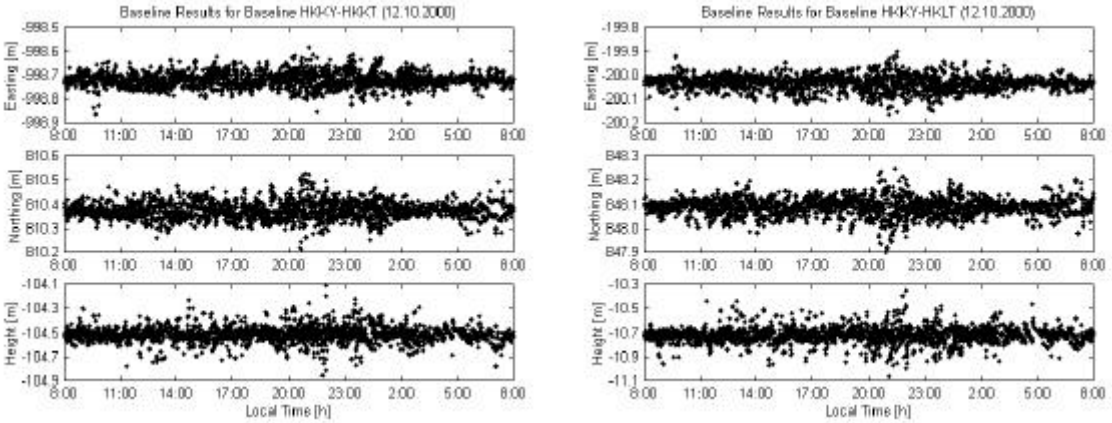

Figure 13: Results for the inner baselines not using ionospheric corrections (DOY 286)

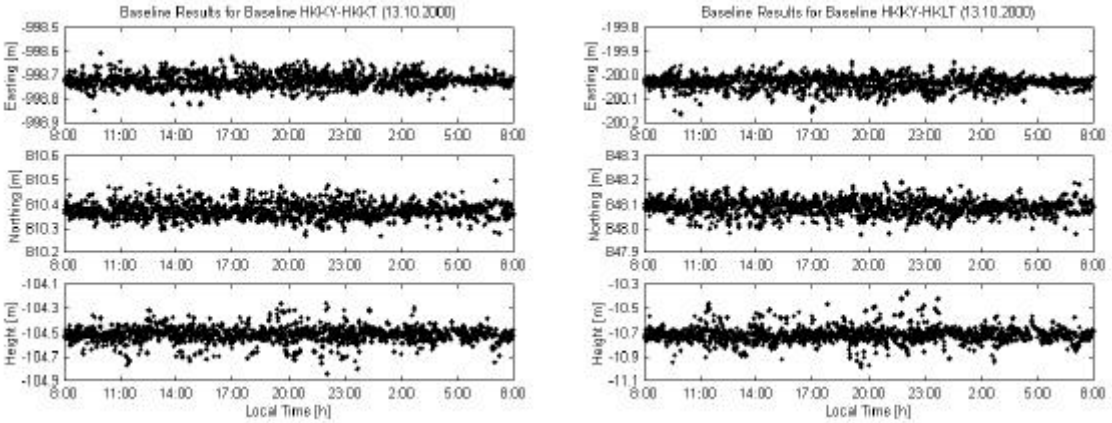

Figure 14: Results for the inner baselines not using ionospheric corrections (DOY 287)

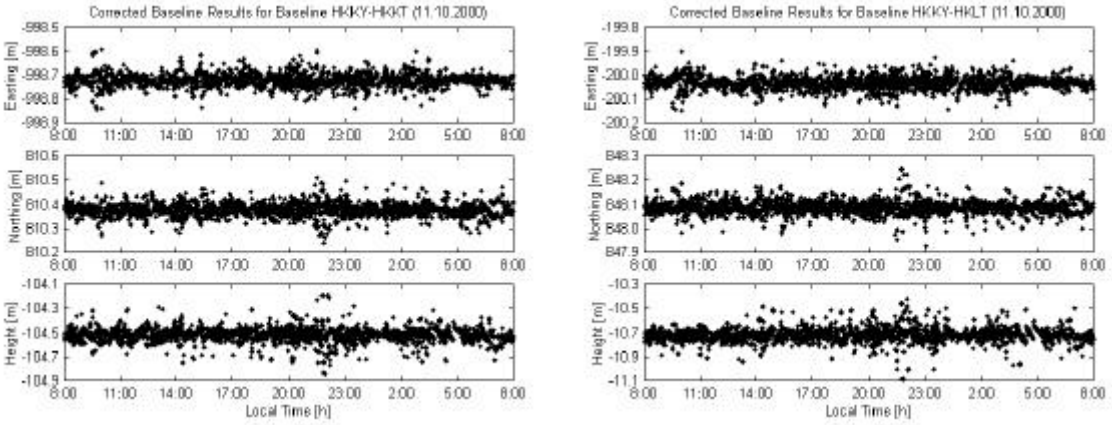

Figure 15: Results for the inner baselines applying ionospheric corrections (DOY 285)

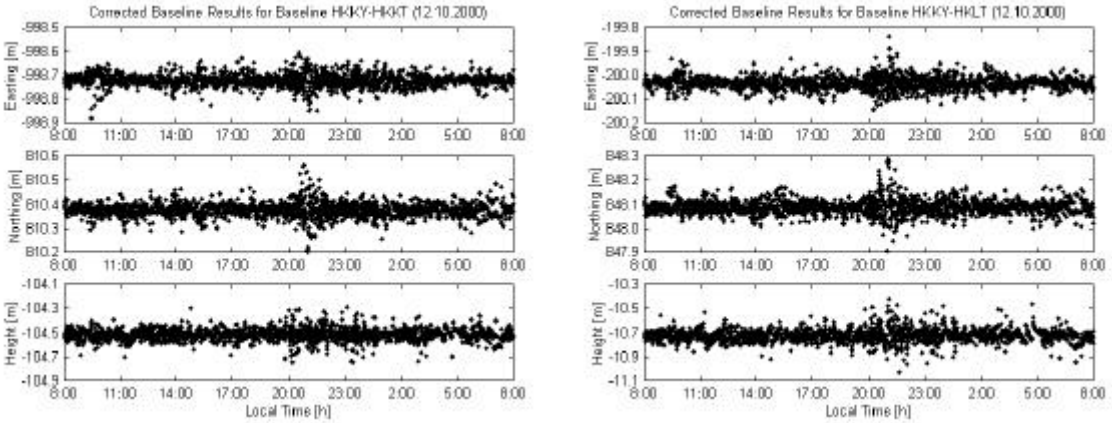

Figure 16: Results for the inner baselines applying ionospheric corrections (DOY 286)

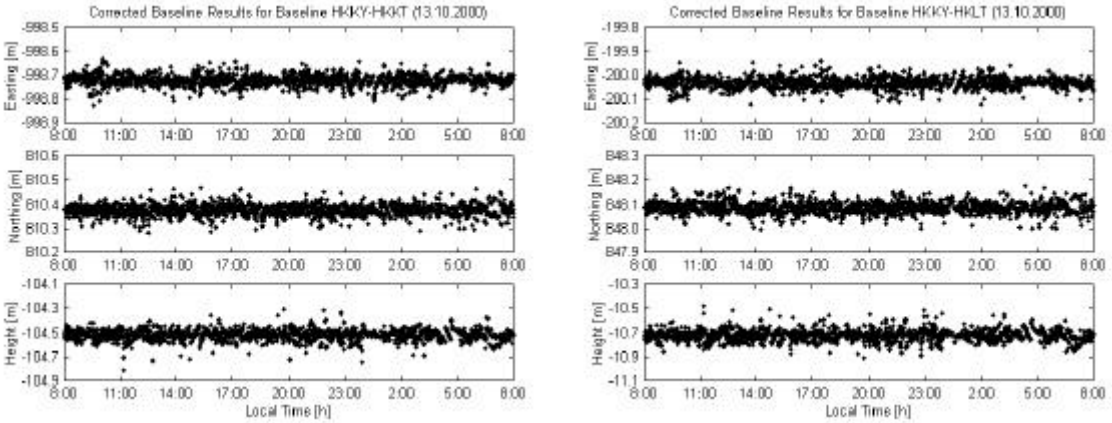

Figure 17: Results for the inner baselines applying ionospheric corrections (DOY 287)

Table 4 lists the standard deviations (STD) of the results obtained for the inner baselines using the two different processing methods (not applying corrections versus applying corrections) on three successive days. Although a comparison of Figures 12-14 and Figures 15-17 does not clearly show this, it is evident that the baseline results are improved by applying the correction terms, as indicated in Table 4. On average, the standard deviation of the baseline results has been reduced by

about 20% in all three components (Table 5). The biggest improvement (of approximately 25%) was achieved on day 287, the day with comparatively calm ionospheric conditions. This indicates that extreme ionospheric conditions, such as those experienced in close proximity to the geomagnetic equator during solar cycle maximum periods, can reduce the efficiency of the proposed method. This is most likely due to short-term effects of the highly variable ionosphere that cannot be modelled adequately. When applying the correction terms, the standard deviations still reach values of 2.0-3.5cm in the horizontal components and 4.5-6.5cm in the height component – values too large to permit reliable detection of ground deformation at the desired accuracy level.

Table 4: Standard deviations of the inner baseline components on days 285-287

	Day 285, no corr.	Day 285, corr.	Day 286, no corr.	Day 286, corr.	Day 287, no corr.	Day 287, corr.
Baseline HKKY-HKKT						
STD Easting [m]	0.02994	0.02578	0.02888	0.02440	0.02738	0.02091
STD Northing [m]	0.03327	0.02635	0.03384	0.02814	0.02927	0.02197
STD Height [m]	0.06150	0.05774	0.06435	0.04770	0.06185	0.04519
Baseline HKKY-HKLT						
STD Easting [m]	0.02957	0.02508	0.02895	0.02452	0.02747	0.02049
STD Northing [m]	0.03265	0.02646	0.03579	0.03136	0.02991	0.02202
STD Height [m]	0.06204	0.05841	0.06526	0.05151	0.06208	0.04578

Table 5: Average improvement in the STD for both baselines on days 285-287

Baseline	DOY	Easting [%]	Northing [%]	Height [%]
HKKY-HKKT (18km)	285	13.9	20.8	6.1
	286	15.5	16.8	25.9
	287	23.6	24.9	26.9
HKKY-HKLT (17km)	285	15.2	19.0	5.9
	286	15.3	12.4	21.1
	287	25.4	26.4	26.3
Average [%]		18	20	19

In a previous study, for a GPS network located in the mid-latitude region and data collected under solar maximum conditions, the standard deviation of the baseline results could be reduced by almost 50% in the horizontal and almost 40% in the vertical component, while standard deviations of less than 1cm horizontally and 1.5-3cm vertically have been achieved for a single-epch baseline solution (Janssen & Rizos, 2002). Unfortunately, in spite of the shorter fiducial baseline lengths, these promising results could not be repeated for this network, situated as it is in the equatorial region. This underlines the significant effect of the ionosphere on GPS deformation monitoring networks, especially at low-latitudes in periods of heightened solar activity.

For baselines involving a significant difference in station altitude, e.g. in GPS volcano deformation monitoring networks, the accuracy could be further improved by estimating an additional residual relative zenith delay parameter to correctly account for the tropospheric bias. Among others, Abidin et al. (1998) and Roberts (2002) state that global troposphere models alone are not sufficient in this case and the relative tropospheric delay has to be estimated and corrected.

5 Conclusions

A procedure to process a mixed-mode GPS network for deformation monitoring applications has been described. Single-frequency GPS observations in the equatorial region have been improved by generating empirical corrections obtained from a fiducial network of dual-frequency reference stations surrounding the inner single-frequency network. This method accounts for the ionospheric bias that otherwise would have been neglected when using single-frequency instrumentation only. Data from the Hong Kong GPS Active Network have been used to simulate such a network

configuration in order to investigate the impact of the proposed processing strategy on the baseline results in a low-latitude region.

The generated correction terms have highlighted that the ionosphere has a significant effect on the GPS baseline results. This effect should not be neglected if it is desired to detect deformational signals with single-frequency instrumentation at a high-accuracy level, especially for networks located in the equatorial region.

The double-differenced correction terms for the inner baselines were derived in two different ways, directly using dual-frequency data and indirectly using the modelling approach. It was shown that the correction generation algorithm proposed in this paper successfully models the correction terms for the inner (single-frequency) baselines.

The results show that very large (of the order of several cycles) ionospheric correction terms are still able to improve the accuracy of the GPS baseline solutions. Hence they do model the ionospheric conditions (at least to some extent). However, due to the severity of the ionospheric conditions the fiducial baselines have to be very short in order to ensure reliable corrections in the equatorial region. A distinct gradient in the ionospheric conditions has been detected with increasing ionospheric effects in the general direction from the southwest to the northeast of the GPS network. The single-frequency baseline repeatability has been improved by applying the empirical correction terms. The standard deviation of the baseline results has been reduced by approximately 20% in all three components. However, the findings also indicate that extreme ionospheric conditions, such as those experienced in close proximity to the geomagnetic equator during solar cycle maximum periods, can reduce the efficiency of the proposed method. This is most likely due to short-term effects that cannot be modelled reliably. The standard deviation of the baseline components for a single-epoch baseline solution could not be reduced below about 2.0-3.5cm horizontally and 4.5-6.5cm vertically. Unfortunately the promising results obtained at mid-latitude sites (see Janssen & Rizos, 2002) could not be repeated for this network, situated as it is in the equatorial region.

Nevertheless, the approach of processing a mixed-mode GPS network described in this paper can be a cost-effective and accurate tool for deformation monitoring suitable for a variety of applications.

Acknowledgements

A/Prof. Peter Morgan from the University of Canberra is thanked for kindly providing the GPS data and precise station coordinates used in this study. The first author is supported in his PhD studies by an International Postgraduate Research Scholarship (IPRS) and funding from the Australian Research Council (ARC).

References

Abidin, H.Z., Meilano, I., Suganda, O.K., Kusuma, M.A., Muhardi, D., Yolanda, O., Setyadji, B., Sukhyar, R., Kahar, J. and Tanaka, T. 1998. Monitoring the Deformation of Guntur Volcano Using Repeated GPS Survey Method. *Proc. XXI Int. Congress of FIG, Commission 5*, Brighton, UK, 19-25 July, 153-169.

Ashkenazi, V., Dodson, A.H., Moore, T. and Roberts, G.W. 1997. Monitoring the Movements of Bridges by GPS. *10th Int. Tech. Meeting of the Satellite Division of the U.S. Inst. of Navigation*, Kansas City, Missouri, 16-19 September, 1165-1172.

Behr, J.A., Hudnut, K.W. and King, N.E. 1998. Monitoring Structural Deformation at Pacoima Dam, California, Using Continuous GPS. *11th Int. Tech. Meeting of the Satellite Division of the U.S. Inst. of Navigation*, Nashville, Tennessee, 15-18 September, 59-68.

Celebi, M. and Sanli, A. 2002. GPS for Recording Dynamic Displacements of Long-Period Structures – Engineering Implications. *2nd Symp. on Geodesy for Geotechnical & Structural Engineering*, Berlin, Germany, 21-24 May, 51-60.

Chen, H.Y., Rizos, C. and Han, S. 2001a. From Simulation to Implementation: Low-Cost Densification of Permanent GPS Networks in Support of Geodetic Applications. *Journal of Geodesy*, 75(9/10), 515-526.

Chen, W., Hu, C., Chen, Y., Ding, X. and Kwok, S.C.W. 2001b. Rapid Static and Kinematic Positioning with Hong Kong GPS Active Network. *14th Int. Tech. Meeting of the Satellite Division of the U.S. Inst. of Navigation*, Salt Lake City, Utah, 11-14 September, 346-352.

Craymer, M.R. and Beck, N. 1992. Session Versus Single-Baseline GPS Processing. *4th Int. Tech. Meeting of the Satellite Division of the U.S. Inst. of Navigation*, Albuquerque, New Mexico, 16-18 September, 995-1004.

Dixon, T.H., Mao, A., Bursik, M., Heflin, M., Langbein, J., Stein, R. and Webb, F. 1997. Continuous Monitoring of Surface Deformation at Long Valley Caldera, California, with GPS. *Journal of Geophysical Research*, 102(B6), 12017-12034.

Han, S. 1997. *Carrier Phase-Based Long-Range GPS Kinematic Positioning*. PhD Dissertation, UNISURV S-49, School of Geomatic Engineering, The University of New South Wales, Sydney, Australia, 185pp.

Han, S. and Rizos, C. 1996. GPS Network Design and Error Mitigation for Real-Time Continuous Array Monitoring Systems. *9th Int. Tech. Meeting of the Satellite Division of the U.S. Inst. of Navigation*, Kansas City, Missouri, 17-20 September, 1827-1836.

Hartinger, H. and Brunner, F.K. 2000. Development of a Monitoring System of Landslide Motions Using GPS. Proc. *9th FIG Int. Symp. on Deformation Measurements*, Olsztyn, Poland, September 1999, 29-38.

Huang, Y.-N. and Cheng, K. 1991. Ionospheric Disturbances at the Equatorial Anomaly Crest Region During the March 1989 Magnatic Storms. *Journal of Geophysical Research*, 96(A8), 13953-13965.

Hudnut, K.W., Bock, Y., Galetzka, J.E., Webb F.H. and Young, W.H. 2001. The Southern California Integrated GPS Network (SCIGN). *10th FIG Int. Symp. on Deformation Measurements*, Orange, California, 19-22 March, 129-148.

IPS 2000. Space Weather and Satellite Communications. Fact sheet, http://www.ips.gov.au/papers/richard/space_weather_satellite_communications.html, 7pp.

Janssen, V. 2001. Optimising the Number of Double-Differenced Observations for GPS Networks in Support of Deformation Monitoring Applications. *GPS Solutions*, 4(3), 41-46.

Janssen, V., Roberts, C., Rizos, C. and Abidin, H.Z. 2001. Experiences with a Mixed-Mode GPS-Based Volcano Monitoring System at Mt. Papandayan, Indonesia. *Geomatics Research Australasia*, 74, 43-58.

Janssen, V. and Rizos, C. 2002. A Mixed-Mode GPS Network Processing Approach for Deformation Monitoring Applications. To appear in *Survey Review*.

Klobuchar, J.A. 1996. Ionospheric Effects on GPS. In: Parkinson, B.W. and Spilker, J.J. (Eds.), *Global Positioning System: Theory and Applications Volume I.* Progress in Astronautics and Aeronautics, 163, American Inst. of Aeronautics and Astronautics, Washington, 485-515.

Meertens, C. 1999. Development of a L1-Phase GPS Volcano Monitoring System – Progress Report for the Period 12 August 1998 – 15 May 1999. http://www.unavco.ucar.edu/~chuckm/l1prog99.pdf.

Mendes, V.B. 1999. *Modeling the Neutral-Atmosphere Propagation Delay in Radiometric Space Techniques*. PhD Dissertation, Dept. of Geodesy & Geomatics Eng. Tech. Rept. No. 199, University of New Brunswick, Fredericton, Canada, 353pp.

Ogaja, C., Rizos, C., Wang, J. and Brownjohn, J. 2001. A Dynamic GPS System for On-line Structural Monitoring. *Int. Symp. on Kinematic Systems in Geodesy, Geomatics & Navigation (KIS 2001)*, Banff, Canada, 5-8 June, 290-297.

Owen, S., Segall, P., Lisowski, M., Miklius, A., Murray, M., Bevis, M. and Foster, J. 2000. January 30, 1997 Eruptive Event on Kilauea Volcano, Hawaii, as Monitored by Continuous GPS. *Geophysical Research Letters*, 27(17), 2757-2760.

Rizos, C. 1997. *Principles and Practice of GPS Surveying*. Monograph 17, School of Geomatic Engineering, The University of New South Wales, Sydney, Australia, 555pp.

Rizos, C., Han, S. and Chen, H.Y. 1998. Carrier Phase-Based, Medium-Range, GPS Rapid Static Positioning in Support of Geodetic Applications: Algorithms and Experimental Results. *Spatial Information Science & Technology (SIST'98)*, Wuhan, P.R. China, 13-16 September, 7-16.

Rizos, C., Han, S., Ge, L., Chen, H.Y., Hatanaka, Y. and Abe, K. 2000. Low-Cost Densification of Permanent GPS Networks for Natural Hazard Mitigation: First Tests on GSI's GEONET Network. *Earth, Planets & Space*, 52(10), 867-871.

Roberts, C. 2002. *A Continuous Low-Cost GPS-Based Volcano Deformation Monitoring System in Indonesia*. PhD Dissertation, School of Surveying and Spatial Information Systems, The University of New South Wales, Sydney, Australia, 287pp.

Saalfeld, A. 1999. Generating Basis Sets of Double Differences. *Journal of Geodesy*, 73, 291-297.

Seeber, G. 1993. *Satellite Geodesy*. de Gruyter, Berlin, Germany, 531pp.

Shimada, S., Fujinawa, Y., Sekiguchi, S., Ohmi, S., Eguchi, T. and Okada, Y. 1990. Detection of a Volcanic Fracture Opening in Japan Using Global Positioning System Measurements. *Nature*, 343, 631-633.

Skone, S.H. 2000. Wide Area Ionosphere Modeling at Low Latitudes – Specifications and Limitations. *13th Int. Tech. Meeting of the Satellite Division of the U.S. Inst. of Navigation*, Salt Lake City, Utah, 19-22 September, 643-652.

Tsuji, H., Hatanaka, Y., Sagiya, T. and Hashimoto, M. 1995. Coseismic Crustal Deformation from the 1994 Hokkaido-Toho-Oki Earthquake Monitored by a Nationwide Continuous GPS Array in Japan. *Geophysical Research Letters*, 22(13), 1669-1672.

Wanninger, L. 1993. Effects of the Equatorial Ionosphere on GPS. *GPS World*, 4(7), 48-54.

Wanninger, L. 1999. The Performance of Virtual Reference Stations in Active Geodetic GPS-Networks under Solar Maximum Conditions. *12th Int. Tech. Meeting of the Satellite Division of the U.S. Inst. of Navigation*, Nashville, Tennessee, 14-17 September, 1419-1427.

Whitaker, C., Duffy, M.A. and Chrzanowski, A. 1998. Design of a Continuous Monitoring Scheme for the Eastside Reservoir in Southern California. *Proc. XXI Int. Congress of FIG, Commission 6*, Brighton, UK, 19-25 July, 329-344.

Wong, K.-Y., Man, K.-L. and Chan, W.-Y. 2001. Monitoring Hong Kong's Bridges – Real-Time Kinematic Spans the Gap. *GPS World*, 12(7), 10-18.

Wu, J.T. 1994. Weighted Differential GPS Method for Reducing Ephemeris Error. *Manuscripta Geodaetica*, 20, 1-7.